International Journal of Thermofluid Science and Technology (2019)
Volume 6, Issue 2, Paper No. 19060201
https://doi.org/10.36963/IJTST.19060201

Research Article

Peristaltic flow of a Jeffery fluid over a porous conduit in the presence of variable liquid properties and convective boundary conditions

G. Manjunatha[1], C. Rajashekhar[1], K. V. Prasad[2], Hanumesh Vaidya[2], Saraswati [2]

[1]*Department of Mathematics, Manipal Institute of Technology, Manipal Academy of Higher Education, Manipal-576104, Karnataka, India*
[2]*Department of Mathematics, Vijayanagara Sri Krishnadevaraya University , Vinayaka Nagar, Ballari-583 105, Karnataka, India*

Received: 21 June 2019; Received in revised form: 10 October 2019; Accepted: 28 October 2019; Published online: 10 November 2019

Abstract

The present article addresses the peristaltic flow of a Jeffery fluid over an inclined axisymmetric porous tube with varying viscosity and thermal conductivity. Velocity slip and convective boundary conditions are considered. Resulting governing equations are solved using long wavelength and small Reynolds number approximations. The closed-form solutions are obtained for velocity, streamline, pressure gradient, temperature, pressure rise, and frictional force. The MATLAB numerical simulations are utilized to compute pressure rise and frictional force. The impacts of various physical parameters in the interims for time-averaged flow rate $\overline{Q}$ with pressure rise $\Delta P > 0$ and $\Delta P < 0$ is examined. The consequences of sinusoidal, multi-sinusoidal, triangular, trapezoidal, and square waveforms on physiological parameters are analyzed and discussed through graphs. The analysis reveals that the presence of variable viscosity helps in controlling the pumping performance of the fluid.

Keywords: Convective conditions; Darcy number; Inclination; Porous tube; Viscosity; Thermal conductivity

1. Introduction

The peristaltic flow is a vital mechanism prompted by the progressive wave of area compression and expansion, which goes along with the walls of the distensible tube or channel. The peristalsis occurs typically in the development of the bolus through the esophagus, urine flow

Corresponding email: hanumeshvaidya@gmail.com(Hanumesh Vaidya)

through the ureter, chyme advancement in the gastrointestinal tract, embryo transport inside the uterine cavity, and the vasomotion of blood in vessels. The researchers have utilized this mechanism to outline a few modern applications, for example, in the nuclear industry, peristaltic pump, roller and finger pumps, transport of destructive and harmful fluids and heart-lung machines. Because of its extensive use in different fields of science, various researchers have investigated the peristaltic transport under a different configuration. Since the greater part of the liquids occurring in industries and physiology behave as a non-Newtonian liquid. Therefore, the examination of the peristaltic transport of non-Newtonian fluid has been of most outrageous centrality to various researchers because of its application in Bioengineering and Medicine (Ramesh and Devakar, 2015; Santosh et al., 2015; Vajravelu et al., 2016; Manjunatha and Rajashekhar, 2018; Rajashekhar et al., 2018). Among the few non-Newtonian models, the Jeffery model is precious because of its vast number of applications in the warm oil recuperation, polymer and sustenance preparing, nourishment and sluttery transportation and the vasomotion of veins. The attempts on the use of the Jeffery model to examine the fluid flow with different configurations can be seen in the literature (Vajravelu et al., 2011, 2014; Sreenadh et al., 2016; Kavitha et al., 2017).

The impact of heat transfer on peristalsis is one of the essential components which has been of extraordinary significance in current circumstances because of its applications in the examination of oxygenation, hemodialysis, and tissues. The variation of temperature fundamentally influences thermal conductivity. Specifically, thermal conductivity is a measure of the limit of a substance to direct heat under typical conditions. This behavior proves that any change in temperature may change the rate at which the material is directing heat. Another fundamental factor that is generously affected by the variation of temperature is convective heat transfer at the boundary. Convective boundary conditions are used to portray a direct convective heat exchange for at least one geometric substance in thermal mode. The examination of the effects of convective boundary conditions assumes a critical part in gas turbines, nuclear plants, and thermal energy storage. Keeping this in mind, Ezzat (1994) examined the unsteady two-dimensional flow with convective boundary conditions through a porous medium. Ezzat and El-Bary (2012) investigated the MHD convectional flow with fractional heat conduction law. Later on, Alsaedi et al. (2013) used convective conditions on the peristaltic flow and also examined the effect of Joule heating. They found that the presence of Joule heating enhances the temperature, and an increase in the estimation of Biot number decreases the temperature. Hayat et al. (2016) extended the work of Alsaedi et al. (2013) by taking Carreau fluid. Further, Sayed et al. (2016) examined the impact of slip and convective boundary conditions on peristaltic transport. Recently, many authors modeled the classical and biological fluid flows by using convective conditions (Srinivas, 2017; Maleque, 2017; Prasad et al., 2018; Mishra et al., 2018; Manjunatha et al., 2019 (a), 2019(b)).

Most of the above studies analyzed the Newtonian/non-Newtonian characteristics of fluid flow by taking constant thermophysical properties of the fluid. These properties may change concerning temperature variation, particularly the variable viscosity and thermal conductivity. For lubricating liquids, the rise in temperature and the heat generated by the inside friction significantly alters the physical properties of the liquid, and therefore these properties are no longer assumed to

be constant. The expansion in temperature prompts an extension in the transport phenomenon; thus the heat exchange at the walls is additionally influenced. The increase in temperature prompts an increment in the transport phenomenon; thus the heat exchange at the walls is furthermore altered.

Consequently, to foresee the flow and heat exchange rates, it is essential to consider the variable liquid properties (Ezzat and Youssef, 2010; Hayat et al., 2014; Abbasi et al., 2015; Hussain et al., 2016; Vaidya et al., 2019 (a), 2019 (b), 2019 (c), 2019 (d)). Subsequently, the supposition of constant viscosity of the liquid neglects to clear up the peristaltic development engaged in the digestive system and the flow of blood in microvessels. In these organs, the viscosity of the liquid differs over the thickness of the channel (Hayat and Ali, 2008; Khan et al., 2013; Lachiheb, 2016; Farroq et al., 2017).

Driven by the above examinations, the present model investigates the impact of variable viscosity and thermal conductivity on the peristaltic stream of a Jeffery liquid in an inclined porous tube with partial slip and convective boundary conditions. The geometry includes the flow through porous media because of its application in bile pipe, filtration of liquids, the human lung, wood, gallbladder, limestone, sandstone, and in the vasomotion of blood in microvessels. In particular, the flow through porous arteries has been of most significance in examining cardiovascular sicknesses and has many industrial applications (Elshehawey and Husseny, 2000; Alsaedi et al., 2014; Sreenadh et al., 2017). The closed-form solutions are obtained by considering the long wavelength and small Reynolds number approximations. Further, the impact of various physiological parameters on velocity, pressure gradient, stream function, pressure rise, frictional force, and temperature are plotted and examined through graphics.

2. Mathematical Modelling and Closed-Form Solutions

We consider a viscous incompressible fluid flow induced by the infinite sinusoidal wave trains moving with velocity c along the walls of an inclined porous tube. The tube is axisymmetric and allows the choice of the cylindrical coordinate system (R,Θ,Z). The viscosity and thermal conductivity are not constant but vary with respect to thickness and temperature, respectively. The r - axis is along the axial direction and z - axis is normal to the axial direction, as shown in Fig.1. The geometry of the tube surface is given by

$$h(z,t)=1+\varepsilon\sin\left(\frac{2\pi}{\lambda}\left[z-ct\right]\right) \tag{1}$$

where ε is the amplitude ratio, λ is the wavelength and t is time.

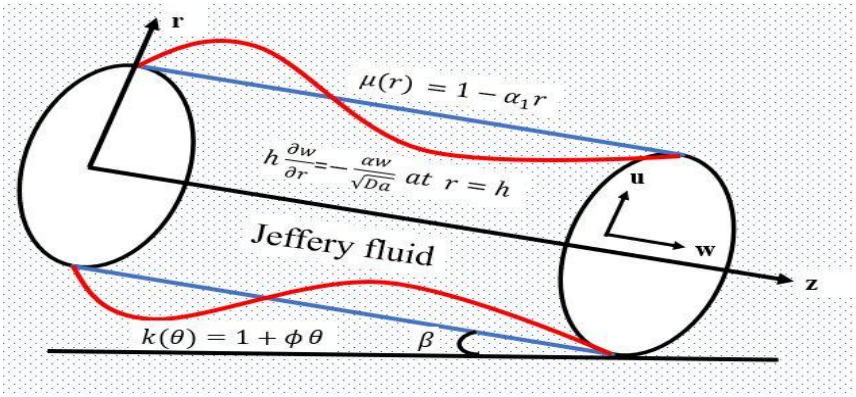

Fig. 1 Geometrical representation of a peristaltic wave in a porous tube.

The governing equation for an incompressible Jeffery fluid are

$$\bar{T} = p\bar{I} + \bar{S}$$

$$\bar{S} = \frac{\mu}{1+\lambda_1}\left(\dot{\gamma} + \lambda_2 \ddot{\gamma}\right) \tag{2}$$

where, $\bar{S}$ is the extra tensor, $\bar{T}$ is the Cauchy's stress tensor, λ_1 is the ratio of relaxation to retardation time, λ_2 is the retardation time, $\bar{I}$ is the identity tensor and γ is the shear rate.

The flow becomes steady in the wave frame (r, θ, z) moving with velocity c away from the fixed frame (R, Θ, Z) given by

$$r = R, \quad z = Z - ct, \quad \psi = \Psi - \frac{R^2}{2}, \quad p(z) = P(Z, t) \tag{3}$$

where p and P are pressures, ψ and Ψ are stream functions in the wave and fixed frames of references, respectively. Utilizing the following non-dimensional quantities,

$$\bar{r} = \frac{r}{a}, \ \bar{z} = \frac{z}{\lambda}, \ \bar{t} = \frac{ct}{\lambda}, \ \bar{p} = \frac{pa^2}{c\lambda\mu_0}, \ \varepsilon = \frac{b}{a}, \ Br = \Pr Ec, \ \bar{u} = \frac{u}{c}, \Pr = \frac{\mu_0 c_p}{k_0}, \ Ec = \frac{c^2}{c_p T_0},$$
$$\mathrm{Re} = \frac{\rho c a}{\mu_0}, F_1 = \frac{\mu_0 c}{\rho g a^2}, \ \overline{\mu(r)} = \frac{\mu(r)}{\mu_0}, \bar{w} = \frac{w}{c}, \ \delta = \frac{a}{\lambda}, \theta = \frac{T - T_0}{T_0}, \quad \bar{\tau} = \frac{\tau}{\mu_0\left(\frac{c}{a}\right)}. \tag{4}$$

The non-dimensional equations of motion and energy in the wave frame of reference, moving with speed *c*, under the lubrication approach is as follows:

$$\mathrm{Re}\,\delta\left(u\frac{\partial}{\partial r} + w\frac{\partial}{\partial z}\right)w = -\frac{\partial p}{\partial z} + \frac{1}{r}\frac{\partial}{\partial r}(r\tau_{rz}) + \delta\frac{\partial}{\partial r}(\tau_{zz}) \tag{5}$$

$$\mathrm{Re}\,\delta^3\left(u\frac{\partial}{\partial r}+w\frac{\partial}{\partial z}\right)u=-\frac{\partial p}{\partial r}+\frac{\delta}{r}\frac{\partial}{\partial r}(r\tau_{rr})+\delta^2\frac{\partial}{\partial r}(\tau_{rz}) \tag{6}$$

$$\begin{aligned}\mathrm{Re}\,\delta\,\mathrm{Pr}\left(u\frac{\partial}{\partial r}+w\frac{\partial}{\partial z}\right)\theta=Ec\,\mathrm{Pr}\left(\delta\frac{\partial u}{\partial r}\tau_{rr}+\frac{\partial w}{\partial r}\tau_{rz}+\delta^2\frac{\partial u}{\partial r}\tau_{zr}+\tau_{zz}\frac{\partial w}{\partial r}\delta\right)\\+\frac{\partial^2\theta}{\partial r^2}+\frac{1}{r}\frac{\partial\theta}{\partial r}+\delta^2\frac{\partial^2\theta}{\partial z^2}\end{aligned} \tag{7}$$

where w and u are the axial and radial velocities, θ is the temperature, Re is the Reynolds number, δ is the wavenumber, Pr is the Prandtl number, Ec is the Eckert number, Br is Brinkman number, r is the radial coordinate and τ is the shear stress.

The variation in viscosity and thermal conductivity is defined as

$$\mu(r)=1-\alpha_1 r,\quad k(\theta)=1+\phi\theta,\quad \text{for } \alpha_1\ll 1 \text{ and } \phi<<1, \tag{8}$$

where α_1 and ϕ are the viscosity and thermal conductivity coefficients respectively.

Under the assumption of long wavelength and small Reynolds number Eqs. (5) – (7) takes the form as

$$\frac{1}{r}\frac{\partial}{\partial r}\left\{\frac{r\mu}{1+\lambda_1}\left(-\frac{\partial w}{\partial r}\right)\right\}=-\frac{\partial p}{\partial z}+\frac{\sin\beta}{F_1} \tag{9}$$

$$0=\frac{\partial p}{\partial r} \tag{10}$$

$$\frac{1}{r}\frac{\partial}{\partial r}\left(r\frac{\partial\theta}{\partial r}\right)=Br\left(-\frac{\partial w}{\partial r}\left[\frac{\mu}{1+\lambda_1}\left\{-\frac{\partial w}{\partial r}\right\}\right]\right) \tag{11}$$

The corresponding non-dimensional slip and convective boundary conditions are (Abbasi et al., 2013; Saffman, 1971)

$$w=-1-\frac{\sqrt{Da}}{\alpha}\frac{\partial w}{\partial r},\quad (1+\phi)\frac{\partial\theta}{\partial r}+Bi\,\theta=0 \text{ at } r=h \tag{12}$$

$$\frac{\partial\theta}{\partial r}=0,\quad \tau_{rz} \text{ is finite at } r=0 \tag{13}$$

For small permeability, the boundary condition proposed by Beavers and Joseph (1961) was simplified by Saffman (1971) and is given in Eq. (12). Physically, this slip corresponds to the fact that there will be no momentum transfer from the fluid layer to the porous layer. Since the porous layer is completely saturated, the momentum instead of penetrating into a porous medium will be converted into a drag by w. This w is the velocity of the fluid at the normal surface and is called the slip velocity (α) at the nominal surface.

The exact solutions are obtained for the velocity expression (9) and (10) satisfying the boundary conditions (12) and (13), we obtain the velocity expression as

$$w = \frac{(P+f)(1+\lambda_1)}{2}\left[\frac{\log(1-\alpha_1 r)}{\alpha_1^2} - \frac{\log(1-\alpha_1 h)}{\alpha_1^2} + \frac{r}{\alpha_1} - \frac{h}{\alpha_1} + \frac{h^2\sqrt{Da}}{\alpha(1-\alpha_1 h)}\right] - 1 \tag{14}$$

Where $P = -\frac{\partial p}{\partial z}$ and $f = \frac{\sin\beta}{F_1}$.

An expression for temperature is obtained by solving equation (11) with the boundary conditions (12) and (13),

$$\theta = \frac{Br(P+f)^2(1+\lambda_1)}{16}\left\{\frac{r^4}{4} - h^3\left(\frac{h}{4} + \frac{1+\phi}{Bi}\right)\right\} \tag{15}$$

The instantaneous volumetric flow rate in the wave frame is given by

$$Q = 2\int_0^h w\, r\, dr \tag{16}$$

$$Q = \frac{(P+f)(1+\lambda_1)}{(\alpha_1 h - 1)}\left[\frac{h}{2\alpha_1^3} - \frac{h^2}{4\alpha_1^2} - \frac{h^3}{12\alpha_1} - \frac{h^4}{6}\left(1 + \frac{3\sqrt{Da}}{\alpha}\right) - \frac{\log(1-\alpha_1 h)}{2\alpha_1^3}\left(h - \frac{1}{\alpha_1}\right)\right] \tag{17}$$

The dimensionless time-averaged flux $\overline{Q}$ across one wavelength is

$$\overline{Q} = \int_0^1\int_0^h r(w-1)\,dr\,dz = q + \int_0^1 h^2\,dz = q + 1 + \frac{\varepsilon^2}{2} \tag{18}$$

The non-dimensional expression for pressure rise (ΔP) and frictional force F across one wavelength is given as follows:

$$\Delta P = \int_0^1 \frac{\partial p}{\partial z}\,dz \tag{19}$$

$$F = \int_0^1 h^2\left(-\frac{\partial p}{\partial z}\right)dz \tag{20}$$

3. Expressions for different waveforms

The non-dimensional expressions for sinusoidal, multi-sinusoidal, triangular, square, and trapezoidal waveforms are as follows:

Sinusoidal wave: $h(z,t) = 1 + \varepsilon\sin\left[\frac{2\pi}{\lambda}(z-t)\right]$ (21)

Multi-Sinusoidal wave: $h(z,t)=1+\varepsilon\sin\left[\frac{2\pi n}{\lambda}(z-t)\right]$ (22)

Triangular wave: $h(z,t)=1+\varepsilon\left[\frac{8}{\pi^3}\sum_{n=1}^{\infty}\frac{(-1)^{n+1}}{(2n-1)^2}\sin\{(2n-1)2\pi(z-t)\}\right]$ (23)

Square wave: $h(z,t)=1+\varepsilon\left[\frac{4}{\pi}\sum_{n=1}^{\infty}\frac{(-1)^{n+1}}{(2n-1)}\cos\{(2n-1)2\pi(z-t)\}\right]$ (24)

Trapezoidal wave: $h(z,t)=1+\varepsilon\left[\frac{32}{\pi^2}\sum_{n=1}^{\infty}\frac{\sin\frac{\pi}{8}(2n-1)}{(2n-1)^2}\sin\{(2n-1)2\pi(z-t)\}\right]$ (25)

4. Results and Discussion

The Eqs. (19) and (20) are numerically integrated by using Weddle's rule in MATLAB. The influence of variable viscosity (α_1), Jeffery parameter (λ_1), porous parameter (Da), slip parameter (α), angle of inclination (β), amplitude ratio (ε), variable thermal conductivity (ϕ), Biot number (Bi) and Brinkmann number (Br) on velocity (w), temperature (θ), pressure rise (ΔP), frictional force (F), pressure gradient (P), time-averaged flow rate $(\overline{Q})$ and streamlines (ψ) are investigated and analyzed through graphs (Figs. 2-11) for the fixed value of $\phi=0.1,\ \lambda_1=0.2,\ \alpha=0.2,\ \alpha_1=0.1,\ \beta=\frac{\pi}{4},\ F_1=0.1,\ t=0.01,\ \varepsilon=0.5,\ Da=0.02, z=0.1,\ Q=0.6,$ $Br=0.25$ and $Bi=0.5$. Further, the quantitative analysis has been done for $\overline{Q}$ where $\Delta P>0$ and $\Delta P<0$ are presented in Tab. I.

4.1 Velocity Field

Fig. 2 illustrates the effects of λ_1, *Da*, α and β on velocity (w). It is observed that the velocity profiles are parabolic in nature with maximum velocity occurs at the center of the tube. Figs. 3(a)-(c) are plotted to examine the effects of λ_1, *Da* and β on velocity. An increase in the value of λ_1, *Da* and β enhances the velocity. The influence of α on velocity shows the opposite behavior as that of λ_1, *Da* and β (Fig. 3(d)). However, in all cases, the presence of variable viscosity plays a vital role in enhancing the velocity.

4.2 Temperature distribution

The behavior of λ_1, *Da*, ϕ, *Bi* and *Br* on θ are demonstrated in Fig. 3. The temperature profiles are non-parabolic and show the dual nature. Fig. 3(a) is graphed to investigate the effect of λ_1 on temperature. An increment λ_1 diminishes the temperature. Fig. 3(b) is sketched to show the

variation of Da on temperature. Here decay in temperature near the axis is due to the higher values of Da and the opposite behavior is noticed near the walls of the tube. The effect of ϕ on temperature is analyzed in Fig. 3(c). Here temperature near the axis of the tube increases for higher values of ϕ and the effect is negligible near the walls. It is because of the reason that the higher value of ϕ allows the liquid to dissipate or absorb heat to its surroundings. Hence, the temperature decreases near the walls of the tube. The effect of Bi on temperature is portrayed in Fig. 3(d). Results indicate that temperature profile is a decreasing function of Bi. Fig. 3(e) elucidates the effect of Br on temperature. With an increment in $Br\,(Ec\times \Pr)$ the resulting temperature enhances. It is because of the viscous dissipation effects present in Ec helps in enhancing the temperature profile. Further, the larger value of $\Pr$ diminishes the thermal conductivity and thereby it enhances the temperature profile.

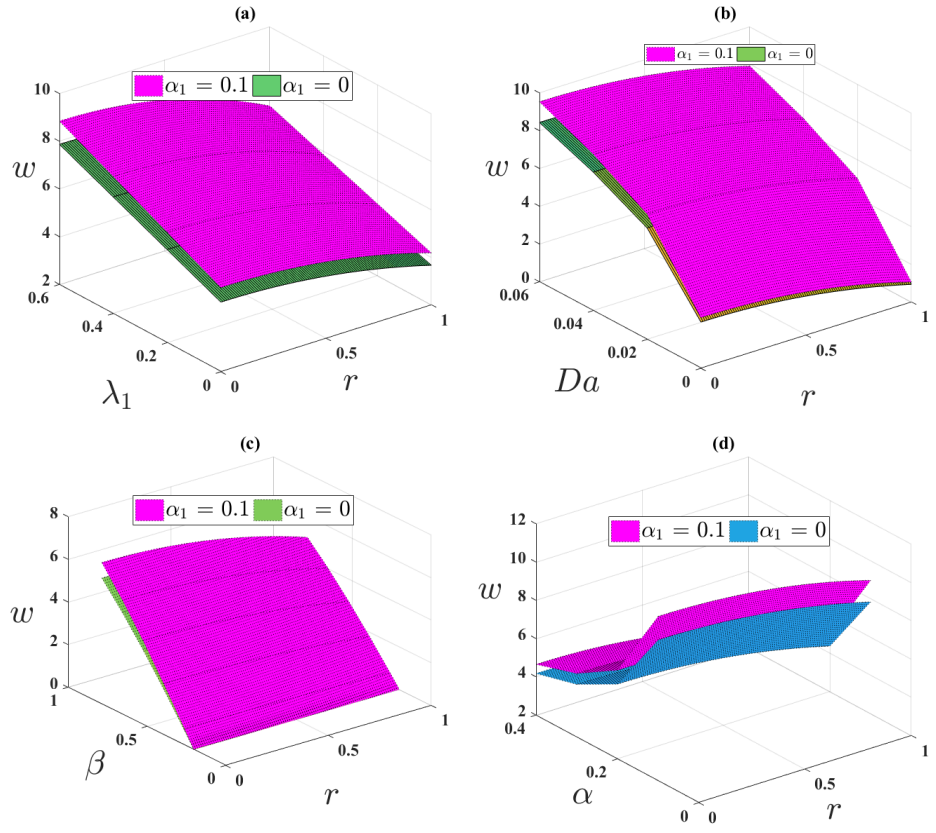

Fig. 2 w versus r for varying (a) Jeffery parameter (λ_1), (b) porous parameter (Da), (c) angle of inclination (β) and (d) velocity slip parameter (α).

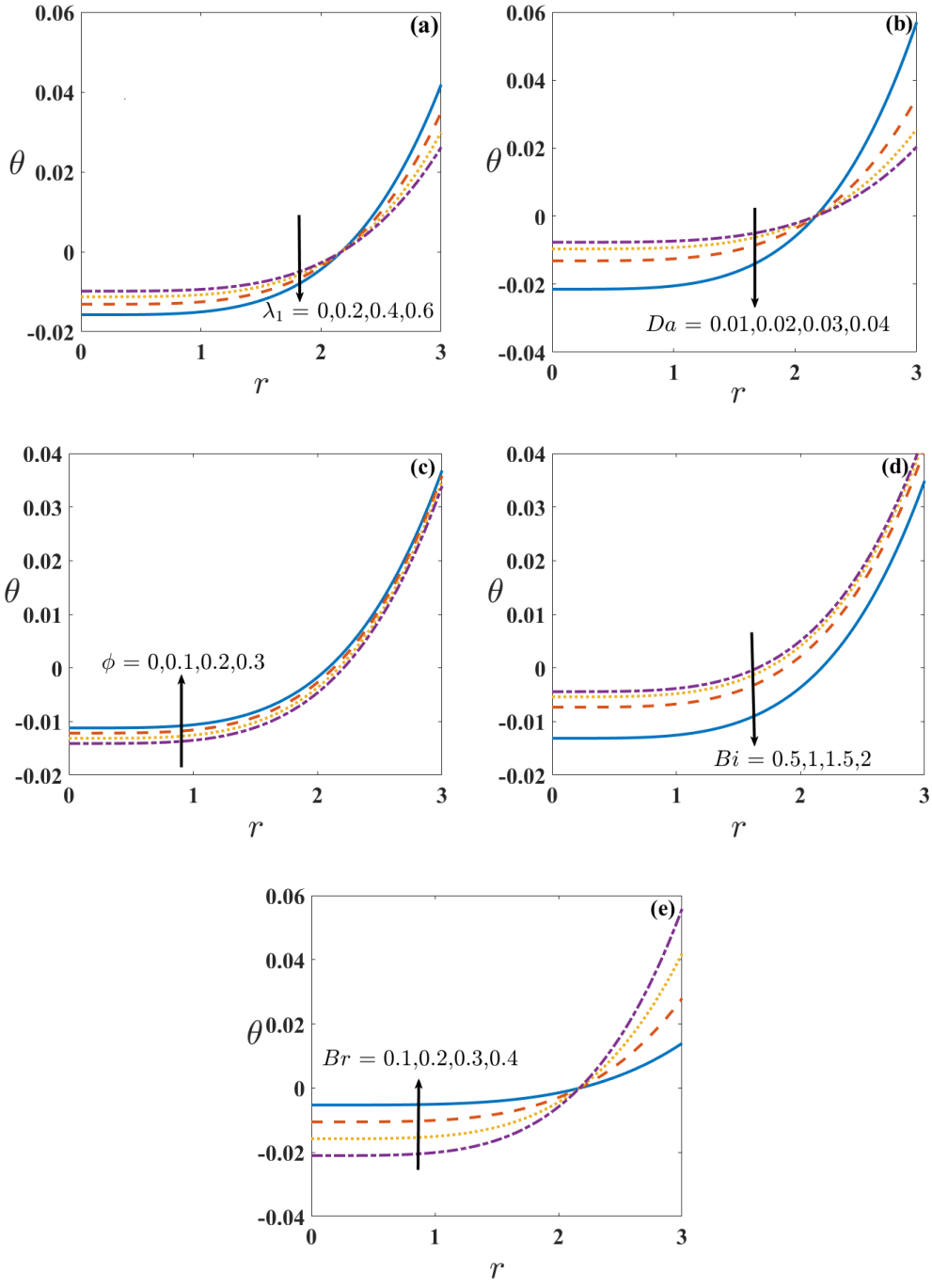

Fig. 3 θ versus r for varying (a) Jeffery parameter (λ_1), (b) porous parameter (Da), (c) thermal conductivity (ϕ), (d) Biot number (Bi) and (e) Brinkmann number (Br).

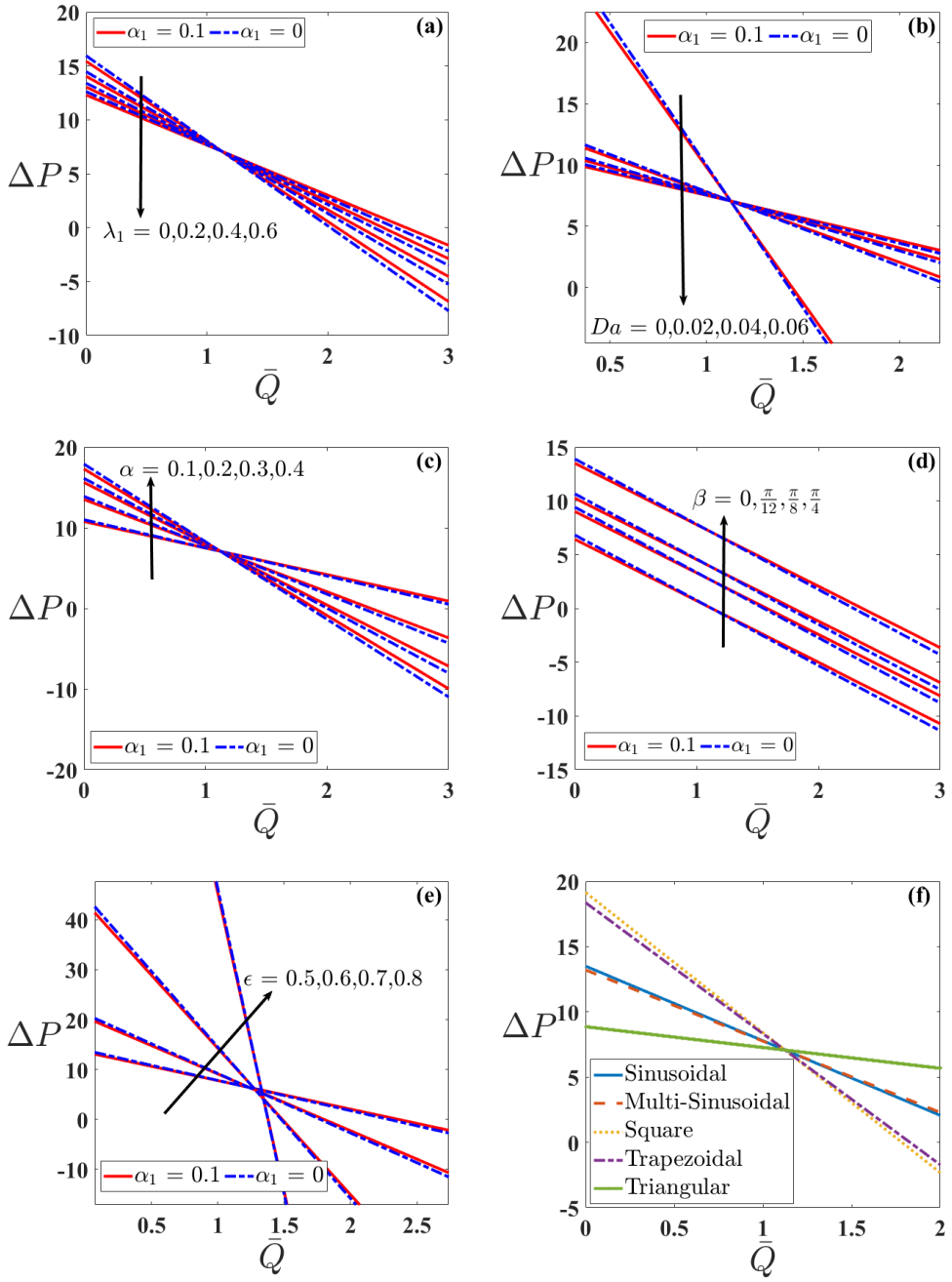

Fig. 4 ΔP versus $\bar{Q}$ for varying (a) Jeffery parameter (λ_1), (b) porous parameter (Da), (c) velocity slip parameter (α), (d) angle of inclination (β), (e) amplitude ratio (ε) and (f) different wave forms.

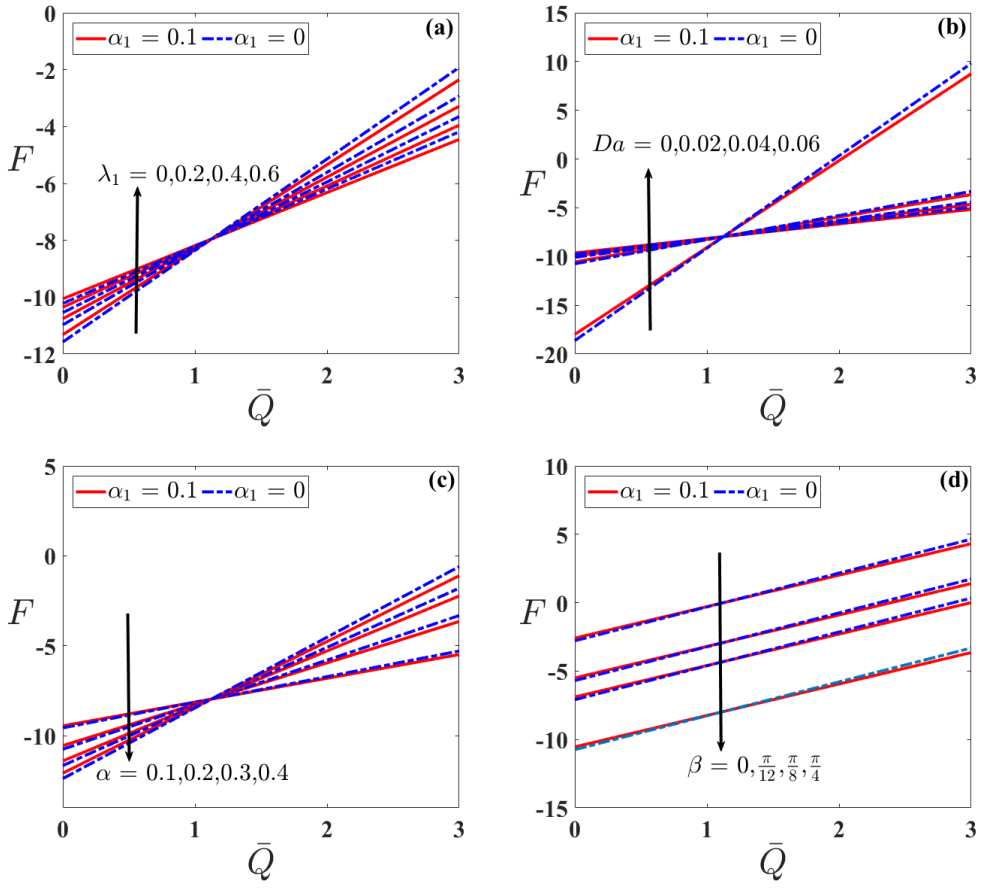

Fig. 5 F versus $\bar{Q}$ for varying (a) Jeffery parameter (λ_1), (b) porous parameter (Da), (c) velocity slip parameter (α) and (d) angle of inclination (β).

4.3 Pumping Characteristics

In the study of peristalsis, pressure rise per wavelength plays a significant role in understanding the physiological behavior of biofluids. This section investigates the influence of variable viscosity and different physiological parameters on pressure rise, friction force, and pressure gradient. The influence of various physiological parameters on pressure rise and the time-averaged flow rate is displayed in Fig.4. It is known that the behavior of many physical parameters is strongly influenced by the range of $\bar{Q}$. Specifically, the impact of physiological parameters shows the opposite behavior before and after a certain critical value of $\bar{Q}$. Fig. 4(a) portrays the variation of λ_1 on ΔP and $\bar{Q}$. Here λ_1 significantly enhances the ΔP in the pumping region $(\Delta P > 0)$ and the corresponding ΔP in the augmented region $(\Delta P < 0)$ diminishes. The pumping profiles for Jeffery fluid $(\lambda_1 \neq 0)$ and Newtonian fluid $(\lambda_1 = 0)$ intersect with each other when $\bar{Q} = 1.1$. This information helps in equalizing the pumping rate of Newtonian and Jeffery

fluid for some value of $\overline{Q}$ by adjusting the peristalsis velocity. Fig. 4(b) illustrates the variation of Da on ΔP and $\overline{Q}$. An increment in Da results in the reduction of ΔP. This is because of an increase in the value of Da increases the porosity of the wall and thus $\overline{Q}$ decreases. Influence of α on ΔP and $\overline{Q}$ are shown in Fig. 4(c). Results indicate that the larger value of α enhances ΔP in the pumping region. Fig. 4(d) reveals that the pressure rise needed for a normal tube $(\beta = 0)$ is less than that of the tube having an angle of inclination. Effect of ε on ΔP and $\overline{Q}$ shows that an increase in the value of ε increases ΔP in a porous tube (See Fig. 4(e)). This is quite physical as the value of ε increases, the corresponding wave height also increases, and thereby, it increases the value of ΔP. Fig. 4(f) is drawn to show the effects of different waveforms such as sinusoidal, multi-sinusoidal, square, trapezoidal and triangular waves on ΔP and $\overline{Q}$. Results indicate that the required value of ΔP is more for the square wave and it is less for the triangular waves when compared with other waveforms. Furthermore, the effects of λ_1, Da, α and β on F and $\overline{Q}$ show the opposite behavior as that of ΔP and $\overline{Q}$ (Fig. 5). To discuss these effects quantitatively the intervals for $\overline{Q}$ where $\Delta P > 0$ and $\Delta P < 0$ are presented in Tab. I. We observe that an increase in the value of λ_1, Da and β increases the length of the interval in the pumping region and opposite behavior is observed in the augmented region. Also, for a fixed value of λ_1, Da and β, the length of the pumping region increases in the case of variable viscosity with that of constant viscosity. Further, the effects of α and ε decrease the length of the interval for $\Delta P > 0$ and opposite behaviour is observed when viscosity increases from 0 to 0.1**.** Fig. 6 is graphed to investigate the influence of λ_1, Da, α and β on P. Here the greatest value of P is observed at the narrowest part of the tube ($z = 0.85$). Further, the positive value of P an adverse pressure gradient is registered (which opposes the flow) in the range $z \in [0.7, 1]$. However, a favorable pressure gradient is seen when P is negative in the interval $z \in [0.5, 0.7]$ and $z \in [1, 1.2]$ which helps the fluid to flow. Figs. 6(a)-(c) are sketched to show the behavior of λ_1, Da and β on P. Here decay in the value of P is subject to increasing values of λ_1, Da and β. Further, the opposite behavior is noticed for larger values of α (Fig. 6(d)). Fig. 7 is plotted to examine the behavior of different waveforms on the pressure gradient. Results show that the value of P is more for square wave and it is found to be less for triangular wave.

4.4 Trapping phenomenon

The essential part of peristalsis is trapping. It is by and large the arrangement of the inside flowing bolus. The movement of the inside flowing bolus in a fluid is implanted by a different stream, which is named as trapping phenomenon. This phenomenon is particularly useful in the movement of thrombus and transport of food bolus in the gastrointestinal tract. Fig. 8 illustrates the effect of Da on trapped bolus. It is noticed that an increase in the value of Da enhances the size of the trapped bolus, and hence, it vanishes for a large value of the porous parameter. Whereas, it diminishes for a larger value of α and ε and thereby increases the number of boluses (Fig. 9

and 10). Fig. 11 demonstrates the impacts of different waveforms on trapped bolus. It is observed that the size of the trapped bolus is small in the case of a triangular wave than the other considered waveforms.

Table 1: Interval for time-averaged flow rate $\overline{Q}$ across one wavelength for different values of the physical parameters when $F_1 = 0.1$ and $t = 0.01$.

α	Da	ε	β	λ_1	$\alpha_1 = 0$		$\alpha_1 = 0.1$	
					$\Delta P > 0$	$\Delta P < 0$	$\Delta P > 0$	$\Delta P < 0$
0.2	0.02	0.5	$\pi/4$	0	$0 < \overline{Q} < 2.022$	$2.022 < \overline{Q} < 3$	$0 < \overline{Q} < 2.179$	$2.179 < \overline{Q} < 3$
				0.2	$0 < \overline{Q} < 2.201$	$2.201 < \overline{Q} < 3$	$0 < \overline{Q} < 2.275$	$2.275 < \overline{Q} < 3$
				0.4	$0 < \overline{Q} < 2.380$	$2.380 < \overline{Q} < 3$	$0 < \overline{Q} < 2.458$	$2.458 < \overline{Q} < 3$
				0.6	$0 < \overline{Q} < 2.559$	$2.559 < \overline{Q} < 3$	$0 < \overline{Q} < 2.648$	$2.648 < \overline{Q} < 3$
0.2	0.02	0.5	0	0.3	$0 < \overline{Q} < 1.126$	$1.126 < \overline{Q} < 3$	$0 < \overline{Q} < 1.126$	$1.126 < \overline{Q} < 3$
			$\pi/12$		$0 < \overline{Q} < 1.552$	$1.552 < \overline{Q} < 3$	$0 < \overline{Q} < 1.578$	$1.578 < \overline{Q} < 3$
			$\pi/8$		$0 < \overline{Q} < 1.756$	$1.756 < \overline{Q} < 3$	$0 < \overline{Q} < 1.795$	$1.795 < \overline{Q} < 3$
			$\pi/4$		$0 < \overline{Q} < 2.291$	$2.291 < \overline{Q} < 3$	$0 < \overline{Q} < 2.362$	$2.362 < \overline{Q} < 3$
0.2	0.02	0.5	$\pi/4$	0.3	$0 < \overline{Q} < 2.291$	$2.291 < \overline{Q} < 3$	$0 < \overline{Q} < 2.362$	$2.362 < \overline{Q} < 3$
		0.6			$0 < \overline{Q} < 1.773$	$1.773 < \overline{Q} < 3$	$0 < \overline{Q} < 1.802$	$1.802 < \overline{Q} < 3$
		0.7			$0 < \overline{Q} < 1.478$	$1.478 < \overline{Q} < 3$	$0 < \overline{Q} < 1.487$	$1.487 < \overline{Q} < 3$
		0.8			$0 < \overline{Q} < 1.378$	$1.378 < \overline{Q} < 3$	$0 < \overline{Q} < 1.379$	$1.379 < \overline{Q} < 3$
0.2	0	0.5	$\pi/4$	0.2	$0 < \overline{Q} < 1.430$	$1.430 < \overline{Q} < 3$	$0 < \overline{Q} < 1.446$	$1.446 < \overline{Q} < 3$
	0.02				$0 < \overline{Q} < 2.291$	$2.291 < \overline{Q} < 3$	$0 < \overline{Q} < 2.362$	$2.362 < \overline{Q} < 3$
	0.04				$0 < \overline{Q} < 2.647$	$2.647 < \overline{Q} < 3$	$0 < \overline{Q} < 2.742$	$2.742 < \overline{Q} < 3$
0.2	0.02	0.5	$\pi/4$	0.3	$0 < \overline{Q} < 2.291$	$2.291 < \overline{Q} < 3$	$0 < \overline{Q} < 2.362$	$2.362 < \overline{Q} < 3$
0.3					$0 < \overline{Q} < 2.004$	$2.004 < \overline{Q} < 3$	$0 < \overline{Q} < 2.057$	$2.057 < \overline{Q} < 3$
0.4					$0 < \overline{Q} < 1.860$	$1.860 < \overline{Q} < 3$	$0 < \overline{Q} < 1.904$	$1.904 < \overline{Q} < 3$

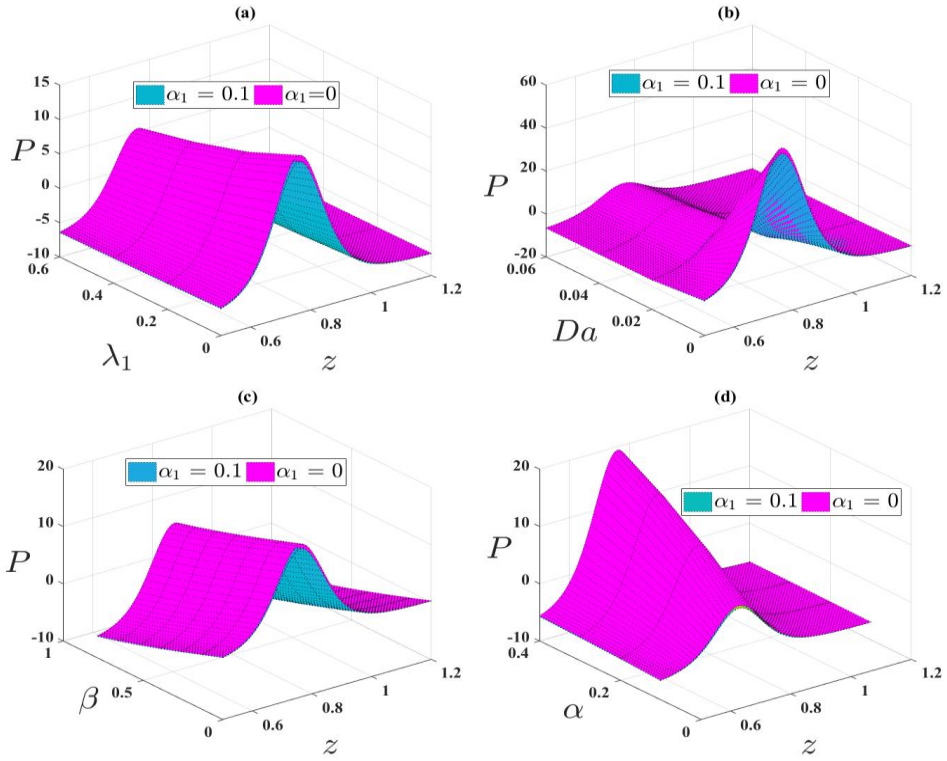

Fig. 6 P versus z for varying (a) Jeffery parameter (λ_1), (b) porous parameter (Da), (c)angle of inclination (β) and (d) velocity slip parameter (α).

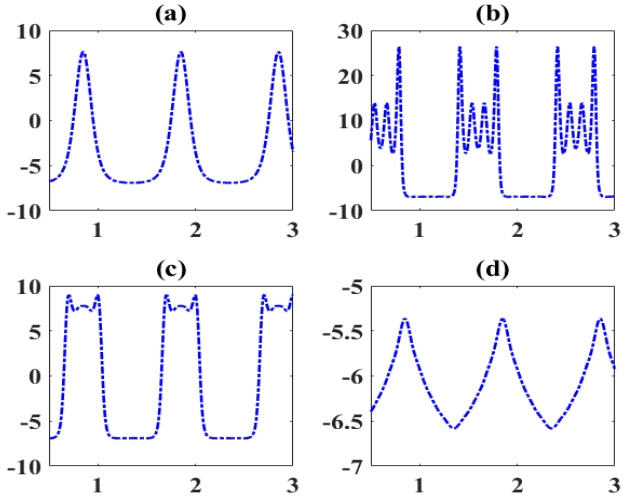

Fig. 7 P versus z for different waveforms (a) Sinusoidal, (b) Square, (c) Trapezoidal and (d) Triangular.

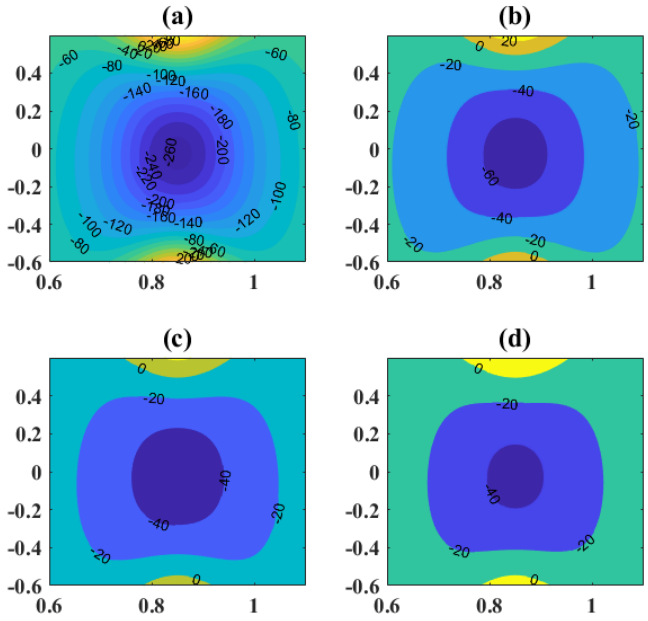

Fig. 8 Streamlines for varying (a) $Da = 0$, (b) $Da = 0.01$, (c) $Da = 0.02$ and (d) $Da = 0.03$.

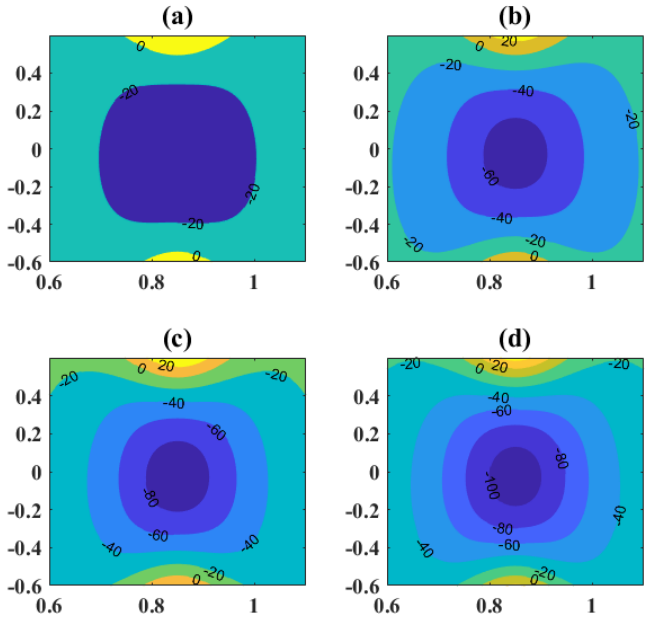

Fig. 9 Streamlines for varying (a) $\alpha = 0.1$, (b) $\alpha = 0.2$, (c) $\alpha = 0.3$ and (d) $\alpha = 0.4$.

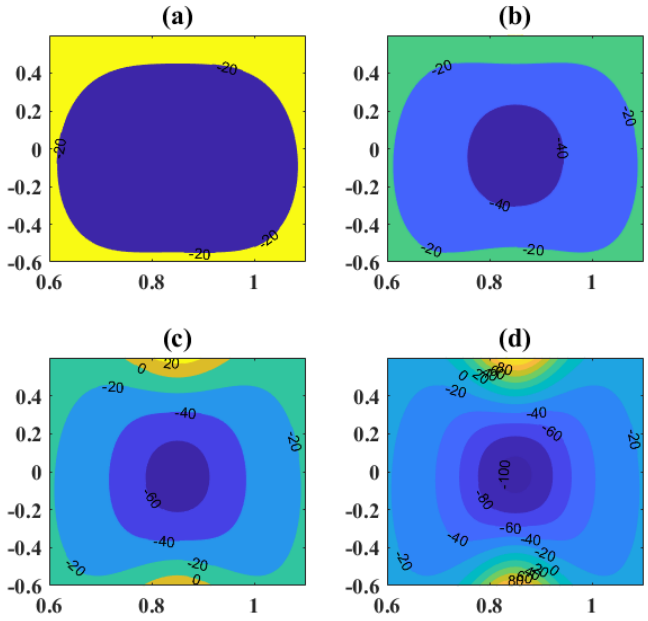

Fig. 10 Streamlines for varying (a) $\varepsilon = 0.3$, (b) $\varepsilon = 0.4$, (c) $\varepsilon = 0.5$ and (d) $\varepsilon = 0.6$.

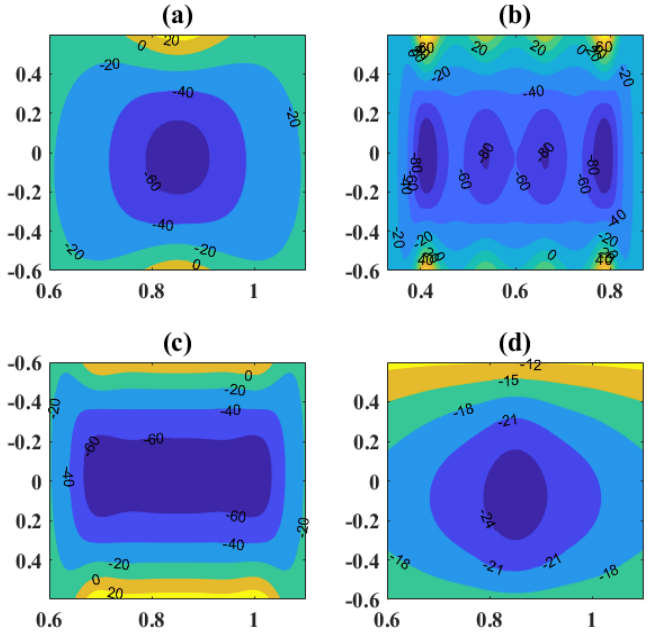

Fig. 11 Streamlines for different wave forms (a) Sinusoidal, (b) Square, (c) Trapezoidal and (d) Triangular.

5. Conclusions

The main findings are as follows:

- The axial velocity field is an increasing function of λ_1, Da and β while it reduces for α.
- The magnitude of temperature decreases for higher Bi.
- There is an increase in temperature near the axis for higher ϕ.
- Pumping performance increases for α and it decreases for λ_1 and β.
- Variable viscosity plays a significant role in controlling pressure rise and temperature.
- The size of trapped bolus increases for Da and it reduces for α.

Acknowledgment

The authors appreciate the constructive comments of the reviewers which led to a definite improvement in the paper.

References

Abbasi, F. M., Hayat, T. & Ahmad, B. (2015). Numerical analysis for peristaltic transport of Carreau-Yasuda fluid with variable thermal conductivity and convective conditions. *Journal of Central South University of Technology*, 22, 4467-4475.

Alsaedi, A., Ali, N., Tripathi, D. & Hayat, T. (2014). Peristaltic flow of couple stress fluid through uniform porous medium, *Applied Mathematics and Mechanics*, 35, 469-480.

Alsaedi, A., Batool, N., Yasmin, H. & Hayat, T. (2013). Convective heat transfer analysis on Prandtl fluid model with peristalsis. *Applied Bionics and Biomechanics*, 10, 197-208.

Beavers, G. S. & Joseph, D. D. (1961). Boundary conditions at a naturally permeable wall. *Journal of Fluid Mechanics*, 30, 197-207.

Elshehawey, E. F. &Husseny, S. Z. A. (2000). Effects of porous boundaries on peristaltic transport through a porous medium.*Acta Mechanica*, 143, 165–177.

Ezzat, M. A. & El-Bary, A. A. (2012). MHD free convection flow with fractional heat conduction law. Magnetohydrodynamics, 48, 587-606.

Ezzat, M. A. & Youssef, M. H. (2010). Stokes' first problem for an electro-conducting micropolar fluid with thermoelectric properties. *Canadian Journal of Physics*, 88, 35-48.

Ezzat, M. M. (1994). State space approach to unsteady two-dimensional free convection flow through a porous medium. *Canadian Journal of Physics*, 72, 311-317.

Farroq, S., Awais, M., Naseem, M., Hayat, T. & Ahmad, B. (2017). Magnetohydrodynamic peristalsis of variable viscosity Jeffery liquid with heat and mass transfer. *Nuclear Engineering and Technology*, 49, 1396-1404.

Hayat, T. & Ali, N. (2008). Effect of variable viscosity on the peristaltic transport of a Newtonian fluid in an asymmetric channel, *Applied Mathematical Modelling*, 32, 761-774.

Hayat, T., Abbasi, F. M., Ahmad, B. &Alsaedi, A. (2014). MHD mixed convection peristaltic flow with variable viscosity and thermal conductivity. *SainsMalaysiana*, 43, 1583-1590.

Hayat, T., Farooq, S., Ahmad, B. &Alsaedi, A. (2016). Characteristics of convective heat transfer in the MHD peristalsis of Carreau fluid with Joule heating. *AIP Advances*, 6, 045302.

Hussain, Q., Asghar, S., Hayat, T. &Alsaedi, A. (2016). Peristaltic transport of hydromagnetic Jeffery fluid with temperature-dependent viscosity and thermal conductivity. *International Journal of Biomathematics*, 9, 1650029.

Kavitha, A., Reddy, R. H., Saravanna, R. & Sreenadh, S. (2017). Peristaltic transport of a Jeffery fluid in contact with a Newtonian fluid in an inclined channel. *Ain Shams Engineering Journal*, 8, 683-687.

Khan, A. A., Ellahi, R. & Usman, M. (2013). The effects of variable viscosity on the peristaltic flow of non-Newtonian fluid through porous medium in an inclined channel with slip boundary conditions. *Journal of Porous Media*, 16, 59-67.

Lachiheb, M. (2016). On the effect of variable viscosity on the peristaltic transport of a Newtonian fluid in an asymmetric channel.*Canadian Journal of Physics*, 94, 320-327.

Maleque, K. A. (2017). Temperature dependent suction/injuction and variable properties on non-Newtonian Casson mixed convective MHD laminar fluid flow with viscous dissipation and thermal radiation. *American Journal of heat and Mass transfer*, 4, 104-120.

Manjunatha, G. & Rajashekhar, C. (2018). Slip effects on peristaltic transport of Casson fluid in an inclined elastic tube with porous walls. *Journal of Advanced Fluid Mechanics and Thermal Sciences*, 43, 67-80.

Manjunatha, G., Rajashekhar, C., Vaidya, H. & Prasad, K.V. (2019) (a). Peristaltic mechanism of Bingham liquid in A convectively heated porous tube in the Presence of variable liquid properties. *Special Topics & Reviews in Porous Media: An International Journal*, 10, 187-201.

Manjunatha, G., Rajashekhar, C., Vaidya, H., Prasad, K.V. & Vajravelu, K. (2019) (b). Impact of heat and mass transfer on the peristaltic mechanism of Jeffrey fluid in a non-uniform porous channel with variable viscosity and variable thermal conductivity. *Journal of Thermal Analysis and Calorimetry*, (2019).

Mishra, J. C., Mallick, B. &. Sinha, A. (2018). Heat and mass transfer in asymmetric channels during peristaltic transport of an MHD fluid having temperature-dependent properties. *Alexandria Engineering Journal*, 57, 391-406.

Rajashekhar, C., Manjunatha, G., Prasad, K. V., Divya, B. B. & Hanumesh Vaidya. (2018). Peristaltic transport of two-layered blood flow using Herschel-Bulkley fluid. *Cogent Engineering*, 5, 1495592.

Ramesh, K &Devakar, M. (2015). Some analytical solutions for flows of Casson fluid with slip boundary conditions. *Ain Shams Engineering Journal*, 6, 967-975.

Saffman, P. G. (1971). On the Boundary conditions at the surface of a porous medium. *Studies in Applied Mathematics*, 50, 93-101.

Santhosh, N., Radhakrishnamacharya, G. &Chamkha, A. J. (2015). Effects of slip on Herschel- Bulkley fluid flow through narrow tubes. *Alexandria Engineering Journal*, 54, 889-896.

Sayed, H. M., Aly, E. H. & Vajravelu, K. (2016). Influence of slip and convective boundary conditions on peristaltic transport of non-Newtonian nanofluids in an inclined asymmetric channel. *Alexandria Engineering Journal*, 55, 2209-2220.

Sreenadh, S., Komala, K. & Srinivas, A. N. S. (2017). Peristaltic pumping of a Power-Law fluid in contact with a Jeffrey fluid in an inclined channel with permeable walls. *Ain Shams Engineering Journal*, 8, 605-611.

Sreenadh, S., Prasad, K. V., Vaidya, H., Sudhakar, E., Gopi Krishna, K. &Krinshnamurty, M. (2016). MHD Couette Flow of a Jeffrey Fluid over a Deformable Porous Layer. International, *Journal of Applied and Computational Mathematics*, 3, 2125-2138.

Srinivasa, R. R. (2017). Application of finite element method to MHD mixed convection chemically reacting flow past a vertical porous plate with cross diffusion and Biot number effects. *American Journal of heat and Mass transfer*, 4, 53-74.

Vaidya, H., Choudhari, R., Gudekote, M. & Prasad, K.V. (2019) (a). Effect of variable liquid properties on peristaltic transport of Rabinowitsch liquid in convectively heated complaint porous channel. *Journal of Central South University*, 26, 1116-1132.

Vaidya, H., Rajashekhar, C., Manjunatha, G. & Prasad, K.V. (2019) (b). Effect of variable liquid properties on peristaltic flow of a Rabinowitsch fluid in an inclined convective porous channel. *The European Physical Journal Plus*, 134, 231.

Vaidya, H., Rajashekhar, C., Manjunatha, G. & Prasad, K.V. (2019) (c). Peristaltic mechanism of a Rabinowitsch fluid in an inclined channel with complaint wall and variable liquid properties. *Journal of the Brazilian Society of Mechanical Sciences and Engineering*, 41, 52.

Vaidya, H., Rajashekhar, C., Manjunatha, G., Prasad, K.V., Makinde, O.D. &Sreenadh, S. (2019) (d). Peristaltic motion of non-Newtonian fluid with variable liquid properties in a convectively heated non-uniform tube: Rabinowitsch fluid model. *Journal of Enhanced Heat Transfer*, 26, 277-294.

Vajravelu, K., Sreenadh, S. &Lakshminarayana, P. (2011). The influence of heat transfer on peristaltic transport of a Jeffrey fluid in a vertical porous stratum. *Communications in Nonlinear Science and Numerical Simulation*, 16, 3107-3125.

Vajravelu, K., Sreenadh, S., Devaki, P & Prasad, K. V. (2016). Peristaltic pumping of a Casson fluid in an elastic tube. *Journal of Applied Fluid Mechanics*. 9, 1897-1905.

Vajravelu, K., Sreenadh, S., Sucharitha, G. &Lakshminarayana, P. (2014). Peristaltic transport of conducting Jeffery fluid in an inclined asymmetric channel. *International Journal of Biomathematics*, 7, 1450064.